Ibn Al-Haitham Journal for Pure and Applied Sciences
Journal homepage: jih.uobaghdad.edu.iq
PISSN: 1609-4042, EISSN: 2521-3407
IHJPAS. 2025, 38(2)

Analysis of Stream Function in a Powell-Eyring Fluid Flow with Couple-Stress Effect and Rotation

Rana Ghazi Ibraheem [1*] and Liqaa Zeki Hummady [2]
[1,2] Department of Mathematics, College of Science, University of Baghdad, Baghdad, Iraq.
*Corresponding Author.

Received: 8 May 2023 Accepted: 21 August 2023 Published: 20 April 2025
doi.org/10.30526/38.2.3478

Abstract

The effect of couple stress, slip condition, changing rotation, and other variables on the peristaltic flow of Powell-Eyring fluid in an inclined asymmetric channel with an inclining magnetic field through a porous media is investigated in this study. Constitutive equations obeying the Powell-Eyring fluid model are employed. In flow analysis, assumptions such as a low Reynolds number and a long wavelength approximation are used. The stream function and mechanical efficiency have closed form expressions devised. The stream function is expressed mathematically. Through the collection of figures, the impact of various criteria is explained and graphically represented Through the collection of figures, the impact has been explained of the Hartman number (Ha), the Darcy number (Da), the inclination of the magnetic field (β), the rotation (Ω), the porous medium parameter (w), the amplitude ratio (ϕ), the slip condition (β_1), and couple stress parameter (α) on stream function have been explained and graphically represented by using the perturbation method which is analytic method. These numerical results were achieved using the mathematical application MATHEMATICA.

Keywords: Couple stress, Magnetic felid, Peristaltic flow, Porous medium, Powell- Eyring fluid.

1. Introduction

Peristaltic pumping is a particular type of pumping that occurs when a variety of complex rheological fluids may be easily transferred between two locations. The term "peristaltic" refers to this method of pumping. The ducts through which the fluid passes undergo intermittent involuntary constriction and then expand. As a result, the pressure gradient rises, causing the fluid to move forward. After Latham's groundbreaking work(1) and because it is utilized in biological, engineering, and physiological systems academics have become increasingly interested in the different applications of peristalsis. Because it is utilized in biological, engineering, and physiological systems, peristaltic transport has received significant attention in recent years. Generally, the peristaltic wave's circular contractions and the successive

longitudinal contractions that occur during peristalsis are generated by the sinuses which propagate along the fluid-containing duct. This technique is the basis for several muscular tubes, including the gastrointestinal tract, fallopian tubes, bile ducts, ureters, esophageal tubes, and others. Peristalsis is used as the basis for the creation of devices such as peristaltic pumps, roller pumps, hose pumps, tube pumps, finger pumps, heart-lung machines, blood pump machines, and dialysis machines. These applications include the transportation of aggressive chemicals, high solid slurries, toxic (nuclear industries), and other materials. Moreover, non-Newtonian fluids are better than numerous industrial and physiological processes that use Newtonian fluids. Among the models of non-Newtonian fluids (which can exhibit various rheological effects), that can be accessed is Powell- Eyring fluid. Although this model is more difficult mathematically than models of non-Newtonian fluids, it deserves more attention because of its distinct benefits. Numerous researchers have been interested in the Powell-Eyring fluid's peristaltic flow mechanism since it was studied by Hina and Mustafa and Hayat and Alsaedi (2), Hayat and Naseema and Rafiq and Fua (3), Hayat and Ahmed (4), Hussain and Alvi and Latif and Asghar (5), and Ali and Liqaa (6). The static magnetohydrodynamic flow and heat transfer of an Eyring-Powell fluid on an expansion plate with viscous dissipation were studied and numerically explained (7). The exchange of thermal energy between different system components is referred to as heat transfer. However, the medium's physical characteristics and the separate compartments' temperatures affect the speed. In recent years, research (8–11) has been conducted about studying the effect of heat transport on non-Newtonian fluids. In a tapered asymmetric channel, the issue of peristaltic transport of an incompressible non-Newtonian fluid is examined (12). With regard to well-established problems of the stir of semi-conductive physiological fluids, such as blood and blood pump machines, magnetic drug forcing, and pertinent methods of human digestion, the advantage of applied magnetic field (MHD) on peristaltic efficacy is crucial (13). It is also helpful in treating gastroparesis, chronic constipation, and morbid obesity as well as magnetic resonance imaging (MRI), which is used to identify brain, vascular diseases, and tumors. A substance that has several tiny holes scattered throughout it is referred to as a porous medium. In riverbeds, fluid infiltration and seepage are sustained by flows over porous media. Important examples of flows through a porous material are those through the ground, water, and oil. Oil is trapped in rock formations like limestone and sandstone, which make up the majority of an oil reservoir (14). Natural porous media can be found in many different forms, such as sand, rye bread, wood, filters, bread loaves, human lungs, and the gallbladder. Food processing, oxygenation, hemodialysis, tissue condition, heat convection for blood flow from tissues' pores, and radiation between the environment and its surface all depend on the action of heat transfer in the peristaltic repositioning of fluid (15–18). Research into fluid peristaltic transfer in the presence of an external magnetic field and rotation is necessary for many issues involving the flow of conductive physiological fluids, such as blood and saline water (19,20). A variety of values are used for the rotational parameters, the porous medium, density, amplitude wave, and taper of the channel, as well as a variety of values for the Hartman number and Darcy number, to study the effects of varying the velocity and pressure gradient. The ability to characterize theologically complicated fluids like liquid crystals and human blood makes the study of pair stress fluid extremely helpful in understanding a variety of physical issues.Couple stress fluid refers to a specific type of non-Newtonian fluid in which the size of the fluid's particles is taken into consideration. Recent researches on the couple stress fluid has been

conducted (21–24). This study's goal is to examine the couple-stress, slip condition, and rotation impacts of Powell-Eyring fluid peristaltic transport in porous media under the combined influence of inclined MHD. Where it was observed that increasing the values of the couple stress coefficient (α) leads to an increase in the size of the bolus trapped and approaching the channel wall, while the increases in the values of rotation (Ω) led to a decrease in the size of the bolus trapped and moving away from the channe walls and when the values of the slip condition (β_1) decrease leading to the decrease in the size of the trapped bolus and moving away from the channel walls.

2. Materials and Methods

2.1. A mathematical formulation for asymmetric flow

Consider the peristaltic motion of an incompressible Powell-Eyring fluid in a two-dimensional, asymmetric conduit with a width of (d'+d). An endless sinusoidal wave traveling along the channel walls at a constant forward speed (c) is what generates flow. The geometry of the wall structure is described as:

$$\overline{h_1}(\bar{x},\bar{t}) = d - a_1 \sin\left[\frac{2\pi}{\lambda}(\bar{X} - c\bar{t})\right] \quad (1)$$

$$\overline{h_2}(\bar{x},\bar{t}) = -d' - a_2 \sin\left[\frac{2\pi}{\lambda}(\bar{X} - c\bar{t}) + \Phi\right] \quad (2)$$

In which $\overline{h_1}(\bar{x},\bar{t})$, $\overline{h_2}(\bar{x},\bar{t})$ are the lower and upper walls respectively, (d, d')denote the channel width, (a_1, a_2) are the amplitudes of the wave, (λ) is the wavelength, (c) is wave the wave speed, (Φ) varies in the range $(0 \le \Phi \le \pi)$, when $\Phi = 0$ is a symmetric channel with out-of-phase waves and $\Phi = \pi$ waves are in phase, the rectangular coordinate system is chosen so that the $\bar{X} - axis$ is in the direction of the wave's motion. and the $\bar{Y} - axis$ perpendicular to $\bar{X}$, where $\bar{t}$ is the time

Further a_1, a_2, d, d' and Φ fulfill the following condition:

$$a_1^2 + a_2^2 + 2a_1a_2\cos\Phi \le (d + d')^2 \quad (3)$$

The Cauchy stress tensor $\bar{\tau}$ for a fluid that obeys the Powell- Eyring model is given as follows:-

$$\bar{\tau} = -PI + \bar{S} \quad (4)$$

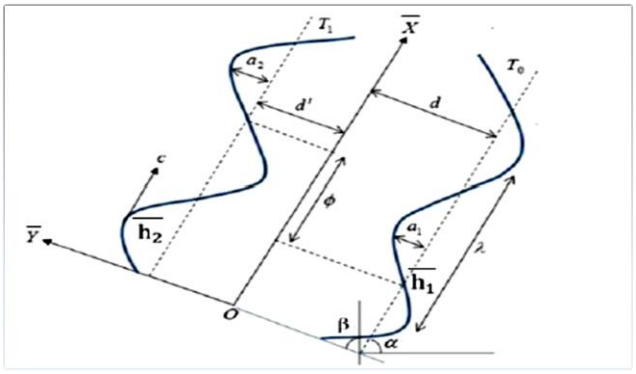

Figure 1. Coordinates for Inclined Asymmetric Channels in Cartesian Space

$$\bar{S} = \left[\mu + \frac{1}{\beta\gamma}\sinh^{-1}\left(\frac{\dot{\gamma}}{c_1}\right)\right] A_{11} \quad (5)$$

$$\dot{\gamma} = \sqrt{\frac{1}{2}\mathrm{tras}(A_{11})^2} \quad (6)$$

$$A_{11} = \nabla\bar{V} + (\nabla\bar{V})^T \quad (7)$$

Where $\bar{S}$ is the extra stress tensor, I is the identity tensor, $\nabla = (\partial\bar{X}, \partial\bar{Y}, 0)$ is the gradient vector,

(β, c_1) are the material parameters of Powell-Eyring fluid, P is the fluid pressure, and μ the dynamic viscosity. The term $\sinh^{-1}$ is approximately equivalent to

$$\sinh^{-1}\left(\frac{\dot{\gamma}}{c_1}\right) = \frac{\dot{\gamma}}{c_1} - \frac{\dot{\gamma}^3}{6{c_1}^3} \quad , \left|\frac{\dot{\gamma}^5}{6{c_1}^5}\right| \ll 1 \tag{8}$$

The flow is governed by three coupled nonlinear partial differentials of continuity, momentum, and energy, which are expressed in frame $(\bar{X}, \bar{Y})$ as

$$\frac{\partial \bar{U}}{\partial \bar{X}} + \frac{\partial \bar{V}}{\partial \bar{Y}} = 0 \tag{9}$$

$$\rho\left(\frac{\partial \bar{U}}{\partial \bar{t}} + \bar{U}\frac{\partial \bar{U}}{\partial \bar{X}} + \bar{V}\frac{\partial \bar{U}}{\partial \bar{Y}}\right) - \rho\Omega\left(\Omega\bar{U} + 2\frac{\partial \bar{V}}{\partial \bar{t}}\right) = -\frac{\partial \bar{P}}{\partial \bar{X}} + \frac{\partial \bar{S}_{\bar{X}\bar{X}}}{\partial \bar{X}} + \frac{\partial \bar{S}_{\bar{X}\bar{Y}}}{\partial \bar{Y}} - \sigma{\beta_0}^2 \cos\beta(\bar{U}\cos\beta - \bar{V}\sin\beta)$$
$$-\frac{\mu}{k}\bar{U} - \mu_1\nabla^4\bar{U} + \rho g \sin\alpha^* \tag{10}$$

$$\rho\left(\frac{\partial \bar{V}}{\partial \bar{t}} + \bar{U}\frac{\partial \bar{V}}{\partial \bar{X}} + \bar{V}\frac{\partial \bar{V}}{\partial \bar{Y}}\right) - \rho\Omega\left(\Omega\bar{V} + 2\frac{\partial \bar{V}}{\partial \bar{t}}\right) = -\frac{\partial \bar{P}}{\partial \bar{Y}} + \frac{\partial \bar{S}_{\bar{X}\bar{Y}}}{\partial \bar{X}} + \frac{\partial \bar{S}_{\bar{Y}\bar{Y}}}{\partial \bar{Y}} - \sigma{\beta_0}^2 \sin\beta(\bar{U}\cos\beta - \bar{V}\sin\beta)$$
$$-\frac{\mu}{k}\bar{V} - \mu_1\nabla^4\bar{V} + \rho g \cos\alpha^* \tag{11}$$

$$\rho C_P\left(\frac{\partial}{\partial \bar{t}} + \bar{U}\frac{\partial}{\partial \bar{X}} + \bar{V}\frac{\partial}{\partial \bar{Y}}\right)\bar{T} = k'\left(\frac{\partial^2}{\partial \bar{t}^2} + \frac{\partial^2}{\partial \bar{X}^2} + \frac{\partial^2}{\partial \bar{Y}^2}\right)\bar{T} + \mu\left[\left(\frac{\partial \bar{U}}{\partial \bar{Y}} + \frac{\partial \bar{V}}{\partial \bar{X}}\right)^2 + 2\left(\frac{\partial \bar{U}}{\partial \bar{X}}\right)^2 + 2\left(\frac{\partial \bar{V}}{\partial \bar{Y}}\right)^2\right] \tag{12}$$

Let $\nabla^2 = \left(\frac{\partial^2}{\partial \bar{X}^2} + \frac{\partial^2}{\partial \bar{X}^2}\right)$ then $\nabla^4 = (\nabla^2)^2$

Where ρ is the fluid density, $\bar{V} = [\bar{U}, \bar{V}]$ is the velocity vector, $\bar{P}$ is the hydrodynamic pressure, $\bar{S}_{\bar{X}\bar{X}}, \bar{S}_{\bar{X}\bar{Y}}, and\ \bar{S}_{\bar{Y}\bar{Y}}$ are the elements of the extra stress tensor $\bar{S}$, σ is the electrical conductivity, β_0 is the constant magnetic field, β is the inclination of the magnetic field, Ω is the rotation C_P is specific heat, k' is the thermal conductivity, $\bar{T}$ is a temperature, and μ for viscosity.

Listed below are the parts of Powell-additional Eying's stress tensor, as described by **Equation (5)**

$$\bar{S}_{\bar{X}\bar{X}} = 2\left(\mu + \frac{1}{\beta C_1}\right)\bar{U}_{\bar{X}} - \frac{1}{3\beta{C_1}^3}\left[2\bar{U}_{\bar{X}}^2 + (\bar{V}_{\bar{X}} + \bar{U}_{\bar{Y}})^2 + 2\bar{V}_{\bar{Y}}^2\right]\bar{U}_{\bar{X}} \tag{13}$$

$$\bar{S}_{\bar{X}\bar{Y}} = 2\left(\mu + \frac{1}{\beta C_1}\right)(\bar{V}_{\bar{X}} + \bar{U}_{\bar{Y}}) - \frac{1}{6\beta{C_1}^3}\left[2\bar{U}_{\bar{X}}^2 + (\bar{V}_{\bar{X}} + \bar{U}_{\bar{Y}})^2 + 2\bar{V}_{\bar{Y}}^2\right](\bar{V}_{\bar{X}} + \bar{U}_{\bar{Y}}) \tag{14}$$

$$\bar{S}_{\bar{Y}\bar{Y}} = 2\left(\mu + \frac{1}{\beta C_1}\right)\bar{V}_{\bar{Y}} - \frac{1}{3\beta{C_1}^3}\left[2\bar{U}_{\bar{X}}^2 + (\bar{V}_{\bar{X}} + \bar{U}_{\bar{Y}})^2 + 2\bar{V}_{\bar{Y}}^2\right]\bar{V}_{\bar{Y}} \tag{15}$$

Natural peristaltic motion is an erratic occurrence, but it applying the transformation from the laboratory frame, stability can be assumed (fixed frame) $(\bar{X}, \bar{Y})$to wave frame (move frame) $(\bar{x}, \bar{y})$. The subsequent transformations determine the connection between pressure, velocities, and coordinates in a laboratory frame $(\bar{X}, \bar{Y})$ to wave frame $(\bar{x}, \bar{y})$

$$\bar{x} = \bar{X} - c, \bar{y} = \bar{Y},\ \bar{u} = \bar{U} - c, \bar{v} = \bar{V},\ \bar{p}(\bar{x}, \bar{y}) = \bar{P}(\bar{X}, \bar{Y}, \bar{t}) \tag{16}$$

Where $\bar{u}$ and $\bar{v}$ represent the velocity factors and $\bar{p}$ represents the pressure in the wave frame. Now that Equation (15) has been substituted into Equation (1), (2), and (9) –(14), the resulting equation has been normalized using the non-dimensional variables shown below:

$$x = \frac{1}{\lambda}\bar{x}, y = \frac{1}{d}\bar{y}, u = \frac{1}{c}\bar{u}, v = \frac{1}{\delta c}\bar{v}, p = \frac{d^2}{\lambda\,\mu\,c}\bar{p}, t = \frac{c}{\lambda}\bar{t}, h_1 = \frac{1}{d}\overline{h_1}, h_2 = \frac{1}{d}\overline{h_2}, \delta = \frac{d}{\lambda}, Re = \frac{\rho\,c\,d}{\mu},$$
$$Ha = d\sqrt{\frac{\sigma}{\mu}}\beta_0, Da = \frac{\bar{k}}{d^2}, w = \frac{1}{\mu\,\beta\,C_1}, A = \frac{w}{6}\left(\frac{C}{C_1\,d}\right)^2,\ \bar{T} = T - T_0, \theta = \frac{T - T_0}{T_1 - T_0},\ Fr = \frac{c^2}{dg}, \beta_1 = \frac{\beta^*}{d},$$
$$S_{xx} = \frac{\lambda}{\mu\,c}\bar{S}_{\bar{X}\bar{X}},\ S_{xy} = \frac{d}{\mu\,c}\bar{S}_{\bar{X}\bar{Y}}, S_{yy} = \frac{d}{\mu\,c}\bar{S}_{\bar{Y}\bar{Y}} \tag{17}$$

Where, (δ) is the wave number, (h_1) and (h_2) are non-dimensional lower and upper wall surfaces respectively, (*Re*) is the Reynolds number, (*Ha*) is the Hartman number, (Φ) is the amplitude ratio, (*w*) is the non-dimensional permeability of the porous medium parameter, (*Da*) is the Darcy number, (*A*) is the Powell-Eyring fluid parameter, (T_0) and (T_1) are the temperatures at the upper and lower walls, (*Fr*) is the Froude number and (α^*) inclination angle of the channel to the

horizontal axis.

Following that is

$$h_1(x,t) = 1 - a\sin(2\pi x),\ a = \frac{a_1}{d} \quad (18)$$

$$h_2(x,t) = -d^* - b\sin(2\pi x + \Phi), b = \frac{a_2}{d}, d^* = \frac{d'}{d} \quad (19)$$

Where a, b, d*, and satisfy Eq.3, then

$$a^2 + b^2 + 2ab\cos\Phi \le (1+d^*)^2 \quad (20)$$

$$\frac{\partial u}{\partial x} + \frac{\partial v}{\partial y} = 0 \quad (21)$$

$$Re\delta\left(\frac{\partial u}{\partial t} + u\frac{\partial u}{\partial x} + v\frac{\partial u}{\partial y}\right) - \frac{\rho d^2\Omega}{\mu}\left(\Omega u + 2\frac{\delta c}{d}\ \frac{\partial v}{\partial t}\right) = -\frac{\partial p}{\partial x} + \delta^2\ \frac{\partial}{\partial x}\ S_{xx} + \frac{\partial}{\partial y}\ S_{xy}$$

$$-Ha^2\cos\beta\ (u\cos\beta - \delta v\sin\beta) - \frac{1}{Da}\ u - \frac{1}{\propto^2}\left(\delta^4\frac{\partial^4}{\partial x^4} + 2\delta^2\frac{\partial^4}{\partial x^2\,\partial y^2} + \frac{\partial^4}{\partial y^4}\right)u +$$

$$\frac{Re}{Fr}\sin\alpha^*(22)Re\delta^3\left(\frac{\partial v}{\partial t} + u\frac{\partial v}{\partial x} + v\frac{\partial v}{\partial y}\right) - \frac{\rho d^2\Omega\delta}{\mu}\left(\Omega\delta v + 2\frac{\delta c}{d}\ \frac{\partial v}{\partial t}\right) = -\frac{\partial p}{\partial x} + \delta^2\ \frac{\partial}{\partial x}\ S_{xy} + \delta\frac{\partial}{\partial y}\ S_{yy}$$

$$+Ha^2\sin\beta\ (\delta u\cos\beta - \delta^2 v\sin\beta) - \delta^2\frac{1}{Da}\ v - \frac{\delta^2}{\propto^2}\left(\delta^4\frac{\partial^4}{\partial x^4} + 2\delta^2\frac{\partial^4}{\partial x^2\,\partial y^2} + \frac{\partial^4}{\partial y^4}\right)v +$$

$$\delta\frac{Re}{Fr}\cos\alpha^* \quad (23)$$

$$Re\delta\left(\frac{\partial\theta}{\partial t} + u\frac{\partial\theta}{\partial x} + v\frac{\partial\theta}{\partial y}\right) = \frac{1}{Pr}\left(c^2\delta^2\frac{\partial^2\theta}{\partial t^2} + \delta^2\frac{\partial^2\theta}{\partial x^2} + \frac{\partial^2\theta}{\partial y^2}\right) + Ec\left[\left(\frac{\partial u}{\partial y} + \delta^2\frac{\partial v}{\partial x}\right)^2 + 2\delta^2\left(\frac{\partial u}{\partial x}\right)^2 + 2\delta^2\left(\frac{\partial v}{\partial y}\right)^2\right] \quad (24)$$

$$S_{xx} = 2(1+w)\frac{\partial u}{\partial x} - 2A\left[2\delta^2\left(\frac{\partial u}{\partial x}\right)^2 + \left(\frac{\partial u}{\partial y} + \delta^2\frac{\partial v}{\partial x}\right)^2 + 2\delta^2\left(\frac{\partial v}{\partial y}\right)^2\right]\frac{\partial u}{\partial x} \quad (25)$$

$$S_{xy} = (1+w)\left(\delta^2\frac{\partial v}{\partial x} + \frac{\partial u}{\partial y}\right) - A\left[2\delta^2\left(\frac{\partial u}{\partial x}\right)^2 + \left(\frac{\partial u}{\partial y} + \delta^2\frac{\partial v}{\partial x}\right)^2 + 2\delta^2\left(\frac{\partial v}{\partial y}\right)^2\right]\left(\delta^2\frac{\partial v}{\partial x} + \frac{\partial u}{\partial y}\right) \quad (26)$$

$$S_{yy} = 2(1+w)\left(\delta\frac{\partial v}{\partial y}\right) - 2A\delta\left[2\delta^2\left(\frac{\partial u}{\partial x}\right)^2 + \left(\frac{\partial u}{\partial y} + \delta^2\frac{\partial v}{\partial x}\right)^2 + 2\delta^2\left(\frac{\partial v}{\partial y}\right)^2\right] \quad (27)$$

In previous equations, Pr is the Prandtl number, Ec is the Eckert number and θ is the dimensionless temperature.

Following are the relations between the stream function (ψ) and velocity components:

$$u = \frac{\partial\Psi}{\partial y}, v = -\frac{\partial\Psi}{\partial x} \quad (28)$$

Substituting Equation (28) into Equations (21) to (270, noting that the mass balance displayed by Equation (21) is similarly satisfied, produces the consequence that Equation (28) is satisfied.

$$Re\ \delta\left(\frac{\partial^2\Psi}{\partial t\,\partial y} + \frac{\partial^3\Psi}{\partial x\,\partial y^2} - \frac{\partial^3\Psi}{\partial x\,\partial y^2}\right) - \frac{\rho d^2\Omega}{\mu}\left(\Omega\frac{\partial\Psi}{\partial y} - 2\frac{\delta c}{d}\ \frac{\partial^2\Psi}{\partial t\,\partial x}\right) = -\frac{\partial p}{\partial x} + \delta^2\frac{\partial}{\partial x}\ S_{xx} + \frac{\partial}{\partial y}S_{xy} -$$

$$Ha^2\cos\beta\left(\frac{\partial\Psi}{\partial y}\ \cos\beta + \delta\frac{\partial\Psi}{\partial x}\sin\beta\right) - \frac{1}{Da}\frac{\partial\Psi}{\partial y} - \frac{1}{\propto^2}\left(\delta^4\frac{\partial^4}{\partial x^4} + 2\delta^2\frac{\partial^4}{\partial x^2\,\partial y^2} + \frac{\partial^4}{\partial y^4}\right)\frac{\partial\Psi}{\partial y} + \frac{Re}{Fr}\sin\alpha^* \quad (29)$$

$$Re\ \delta^3\left(-\frac{\partial^2\Psi}{\partial t\,\partial x} - \frac{\partial^3\Psi}{\partial x^2\,\partial y} - \frac{\partial^3\Psi}{\partial x^2\,\partial y}\right) - \frac{\rho d^2\Omega\delta}{\mu}\left(-\Omega\delta\frac{\partial\Psi}{\partial x} - 2\frac{\delta c}{d}\ \frac{\partial^2\Psi}{\partial t\,\partial x}\right) = -\frac{\partial p}{\partial y} + \delta^2\frac{\partial}{\partial x}\ S_{xy} + \delta\frac{\partial}{\partial y}S_{yy} +$$

$$Ha^2\sin\beta\left(\delta\frac{\partial\Psi}{\partial y}\ \cos\beta + \delta^2\frac{\partial\Psi}{\partial x}\sin\beta\right) + \delta^2\frac{1}{Da}\frac{\partial\Psi}{\partial x} + \frac{\delta^2}{\propto^2}\left(\delta^4\frac{\partial^4}{\partial x^4} + 2\delta^2\frac{\partial^4}{\partial x^2\,\partial y^2} + \frac{\partial^4}{\partial y^4}\right)\frac{\partial\Psi}{\partial x} +$$

$$\delta\frac{Re}{Fr}\cos\alpha^*\ 9 \quad (30)$$

$$\mathrm{Re}\delta\left(\frac{\partial\theta}{\partial t}+\frac{\partial\Psi}{\partial y}\frac{\partial\theta}{\partial x}-\frac{\partial\Psi}{\partial x}\frac{\partial\theta}{\partial y}\right)=\frac{1}{\mathrm{Pr}}\left(c^2\delta^2\frac{\partial^2\theta}{\partial t^2}+\delta^2\frac{\partial^2\theta}{\partial x^2}+\frac{\partial^2\theta}{\partial y^2}\right)+\mathrm{Ec}\left[\left(\frac{\partial^2\Psi}{\partial y^2}+\delta^2\frac{\partial^2\Psi}{\partial x^2}\right)^2+2\delta^2\left(\frac{\partial^2\Psi}{\partial x\,\partial y}\right)^2+2\delta^2\left(\frac{\partial^2\Psi}{\partial x\,\partial y}\right)^2\right] \quad (31)$$

$$S_{xx}=2(1+w)\frac{\partial^2\Psi}{\partial x\,\partial y}-2A\left[2\delta^2\left(\frac{\partial^2\Psi}{\partial x\,\partial y}\right)^2+\left(\frac{\partial^2\Psi}{\partial y^2}-\delta^2\frac{\partial^2\Psi}{\partial x^2}\right)^2+2\delta^2\left(\frac{\partial^2\Psi}{\partial x\,\partial y}\right)^2\right] \quad (32)$$

$$S_{xy}=(1+w)\left(-\delta^2\frac{\partial^2\Psi}{\partial x^2}+\frac{\partial^2\Psi}{\partial y^2}\right)-A\left[2\delta^2\left(\frac{\partial^2\Psi}{\partial x\,\partial y}\right)^2+\left(-\delta^2\frac{\partial^2\Psi}{\partial x^2}+\delta^2\frac{\partial\Psi}{\partial y^2}\right)^2+2\delta^2\left(\frac{\partial^2\Psi}{\partial x\,\partial y}\right)^2\right]\left(-\delta^2\frac{\partial^2\Psi}{\partial x^2}+\frac{\partial^2\Psi}{\partial y^2}\right) \quad (33)$$

$$S_{yy}=-2(1+w)\delta\frac{\partial^2\Psi}{\partial x\,\partial y}-2A\delta\left[2\delta^2\left(\frac{\partial^2\Psi}{\partial x\,\partial y}\right)^2+\left(\frac{\partial^2\Psi}{\partial y^2}-\delta^2\frac{\partial^2\Psi}{\partial x^2}\right)^2+2\delta^2\left(\frac{\partial^2\Psi}{\partial x\,\partial y}\right)^2\right]\left(-\frac{\partial^2\Psi}{\partial x\,\partial y}\right) \quad (34)$$

Now, the Equations (29- 34) become the form when ($Re\ and\ \delta \ll 1$) are present:

$$-\frac{\rho d^2\Omega^2}{\mu}\frac{\partial\Psi}{\partial y}=-\frac{\partial p}{\partial x}+\frac{\partial}{\partial y}S_{xy}-\left(\mathrm{Ha}^2\cos^2\beta+\frac{1}{\mathrm{Da}}\right)\frac{\partial\Psi}{\partial y}-\frac{1}{\propto^2}\frac{\partial^5\Psi}{\partial y^5}+\frac{\mathrm{Re}}{\mathrm{Fr}}\sin\alpha^* \quad (35)$$

$$-\frac{\partial p}{\partial y}=0 \quad (36)$$

$$\frac{\partial^2\theta}{\partial y^2}=-\mathrm{Ec.Pr}\left(\frac{\partial^2\Psi}{\partial y^2}\right)^2 \quad (37)$$

While the component of the extra stress tensor becomes the form of

$$S_{xx}=2(1+w)\frac{\partial^2\Psi}{\partial x\,\partial y}-2A\left(\frac{\partial^2\Psi}{\partial y^2}\right)^2\frac{\partial^2\Psi}{\partial x\,\partial y} \quad (38)$$

$$S_{xy}=(1+w)\left(\frac{\partial^2\Psi}{\partial y^2}\right)-A\left(\frac{\partial^2\Psi}{\partial y^2}\right)^3 \quad (39)$$

$$S_{yy}=0 \quad (40)$$

Also, if Equation (39) is entered into Equation (35) as well as the derivative with respect to y and by (w+1) is taken, then the following equation is obtained:

$$\frac{\partial^4\Psi}{\partial y^4}-\eta A\frac{\partial^2}{\partial y^2}\left(\frac{\partial^2\Psi}{\partial y^2}\right)^3-\zeta\frac{\partial^2\Psi}{\partial y^2}-\eta\frac{1}{\propto^2}\frac{\partial^6\Psi}{\partial y^6}=0 \quad (41)$$

Where

$$\zeta=\frac{\mathrm{Ha}^2\cos^2\beta+\frac{1}{\mathrm{Da}}-\frac{\rho d^2\Omega^2}{\mu}}{w+1},\ \eta=\frac{1}{w+1}$$

$$\Psi=\frac{F}{2}\ ,\frac{\partial\Psi}{\partial y}=-1\ ,\theta=0\quad \text{at}\quad y=h_1\ ,\Psi=-\frac{F}{2}\ ,\frac{\partial\Psi}{\partial y}=-1\ ,\theta=0\quad \text{at}\quad y=h_2 \quad (42)$$

$$\frac{\partial\Psi}{\partial y}+\beta_1\frac{\partial^2\Psi}{\partial y^2}=-1\ \ \text{at}\ y=h_1\ \ ,\frac{\partial\Psi}{\partial y}+\beta_1\frac{\partial^2\Psi}{\partial y^2}=-1\ \ \text{at}\ y=h_2 \quad (43)$$

$$\frac{\partial^3\Psi}{\partial y^3}=0\ \ \text{at}\ y=h_1\ \ ,\frac{\partial^3\Psi}{\partial y^3}=0\ \ \text{at}\ y=h_2 \quad (44)$$

In the wave frame, the dimensionless volume flow rate and boundary condition are as follows:

F represents the dimensionless temporal average flow in the wave frame. Through the expression, it is related to the dimensionless temporal mean flow rate (Q) in the laboratory frame

$$Q=F+1+d^* \quad (45)$$

2.2.Effect of a couple – stress

In this part, a relationship between the pair stress parameter (α) and the material fluid parameters (A) would be found. The relationship will help us in simplifying the problem's solution. Because of the use of the perturbation method in solving the stream function, and to see the impact of every parameter contained in the problem, the zero and first-order solutions must be found. However,

we just need to find the zero-order utilizing the relationship between the pair stress parameter and the material fluid properties. Fluid parameters from a substance with no dimensions:

Let $\mathrm{A} = \frac{\mathrm{w}}{6}\left(\frac{\mathrm{c}}{\mathrm{c_1 d}}\right)^2$

Then

$$d = \sqrt{\frac{w}{6A}}\left(\frac{c}{c_1}\right) \tag{46}$$

Since

$$\alpha = d\sqrt{\frac{\mu}{\mu_1}} \tag{47}$$

Substitute Equation (46) into Equation (47), we get

$$\alpha = \sqrt{\frac{\mathrm{w}\mu}{6\mathrm{A}\mu_1}}\left(\frac{\mathrm{c}}{\mathrm{c_1}}\right) \tag{48}$$

$$\alpha^2 = \frac{w\mu}{6A\mu_1}\left(\frac{c}{c_1}\right)^2 \quad \text{and} \quad \frac{1}{\alpha^2} = \frac{6A\mu_1}{w\mu}\left(\frac{c_1}{c}\right)^2 \tag{49}$$

2.3.Solution of the problem

By using Equation (45) with Equations (35 – 40) and boundary conditions (42 – 44) and since $\delta \leq 1$, and using the approximation of a long wavelength and a low Reynolds number. For the appearance of the couple stress parameter in the equation, the solution is limited to the zero order by giving all the parameters required to solve the problem and find the results, we get the motion equation in terms of stream function which is

$$\boldsymbol{\Psi_{yyyy} - \zeta\Psi_{yy} - \frac{\eta}{\alpha^2}\Psi_{yyyyyy} = 0} \tag{50}$$

The straight forward formula for the momentum equation's solution is

$$\Psi = \sqrt{2}\left(\frac{\sqrt{2}\mathrm{e}^{\mathrm{p1}y}\mathrm{C1}}{\mathrm{p3}} + \frac{\sqrt{2}\mathrm{e}^{-\mathrm{p1}y}\mathrm{C2}}{\mathrm{p3}} + \frac{\sqrt{2}\mathrm{e}^{\mathrm{p2}y}\mathrm{C3}}{\mathrm{p4}} + \frac{\sqrt{2}\mathrm{e}^{-\mathrm{p2}y}\mathrm{C4}}{\mathrm{p4}}\right) + \mathrm{C5} + y\mathrm{C6\ b} \tag{51}$$

Where

$$\mathrm{p1} = \frac{\sqrt{\frac{\alpha^2 - \sqrt{\alpha^2(\alpha^2 - 4\zeta\eta)}}{\eta}}}{\sqrt{2}}$$

$$\mathrm{p2} = \frac{\sqrt{\frac{\alpha^2 + \sqrt{\alpha^2(\alpha^2 - 4\zeta\eta)}}{\eta}}}{\sqrt{2}}$$

$$\mathrm{p3} = \sqrt{\frac{\alpha^2 - \sqrt{\alpha^2(\alpha^2 - 4\zeta\eta)}}{\eta}}\sqrt{\frac{\alpha^2 - \sqrt{\alpha^4 - 4\alpha^2\zeta\eta}}{\eta}}$$

$$\mathrm{p4} = \sqrt{\frac{\alpha^2 + \sqrt{\alpha^2(\alpha^2 - 4\zeta\eta)}}{\eta}}\sqrt{\frac{\alpha^2 + \sqrt{\alpha^4 - 4\alpha^2\zeta\eta}}{\eta}}$$

Within the fixed frame, the axial velocity component is expressed as

$$u(x, y, t) = \Psi_{\mathrm{y}} \tag{52}$$

Now, substitute equation (39) into equation (35), we get

$$\frac{\partial p}{\partial x} = (w+1)\Psi_{yyy} - (w+1)\zeta\Psi_y - \frac{1}{\alpha^2}\Psi_{yyyyy} + \frac{Re}{Fr}\sin\alpha^* \tag{53}$$

3. Results and discussions

This section displays the stream function by using the MATHEMATICA software. A fascinating occurrence happens in peristaltic flows, where the closed stream function traps a quantity of fluid sometimes referred to as bolus inside the channel adjacent to walls, and moves in

the direction of wave propagation. The stream function is plotted for various values of the Hartman number (Ha), the Darcy number (Da), the inclination of the magnetic field (β), the rotation (Ω), the values of the porous medium parameter (w), the amplitude ratio (ϕ), the slip condition (β_1), and the couple stress parameter (α) in the asymmetric channels illustrated in **Figures (2-9)**.

- **Figures (2, 4** and **9)** display the increases in the values of Hartman number (*Ha*), the inclination of magnetic field (β), and the couple stress parameter (α) leading to the increase in the size of the trapped bolus and approaching to the channel walls.
- **Figures (5 , 6)** illustrate the increases in the values of the rotation (Ω) and the values of the porous medium parameter (w) led to the decrease in the size of the trapped bolus and the move away from the channel walls.
- **Figure 3** demonstrates how the confined bolus's size has increased and its approach from the channel wall is caused by a drop in the values of the Darcy number (Da).
- **Figures (7 , 8)** show how decreasing values of the amplitude ratio (ϕ) and the slip condition (β_1) caused the trapped bolus to shrink and move away from the channel walls.

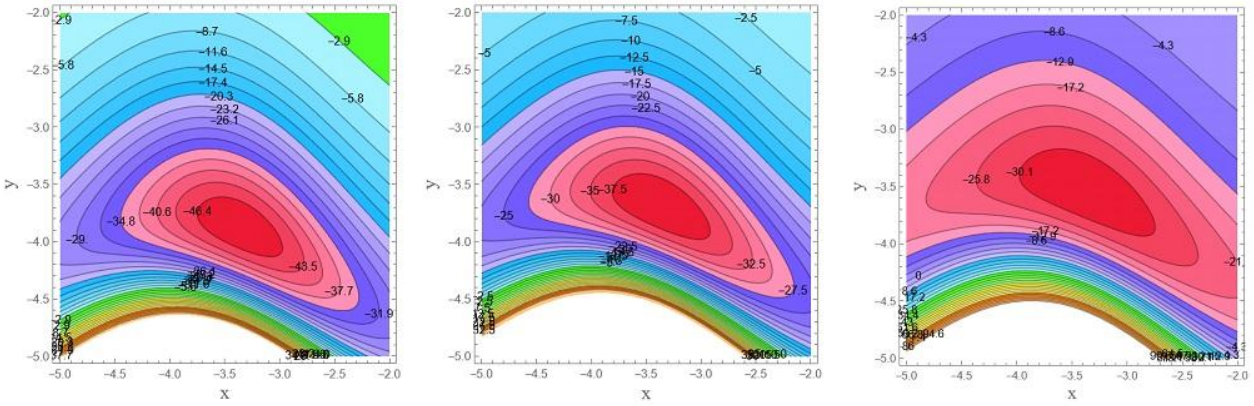

Figure 2. Stream function variation for different (a) Ha=7.5, (b) Ha=8, (c) Ha=8.5 when, $\beta = 2.5, \mathrm{Da} = 10, \rho = 0.7, d = 5, \Omega = 1.5, \mu = 3, w = 0.01, \phi = 2.5, a = 0.4, b = 0.6, d_1 = 0.5, F_\circ = 0.9, \beta_1 = 4, \alpha = 0.6$

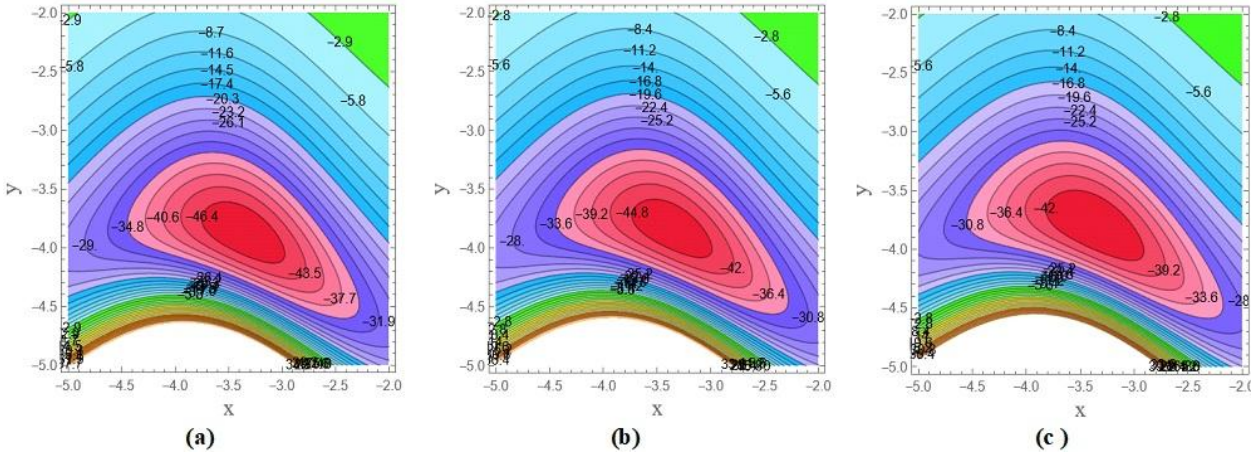

Figure 3. Stream function variation for different (a) Da=10, (b) Da=1, (c) Da=0.5 when $\mathrm{Ha} = 7.5, \beta = 2.5, \rho = 0.7, d = 5, \Omega = 1.5, \mu = 3, w = 0.01, \phi = 2.5, a = 0.4, b = 0.6, d_1 = 0.5, F_\circ = 0.9, \beta_1 = 4, \alpha = 0.6$

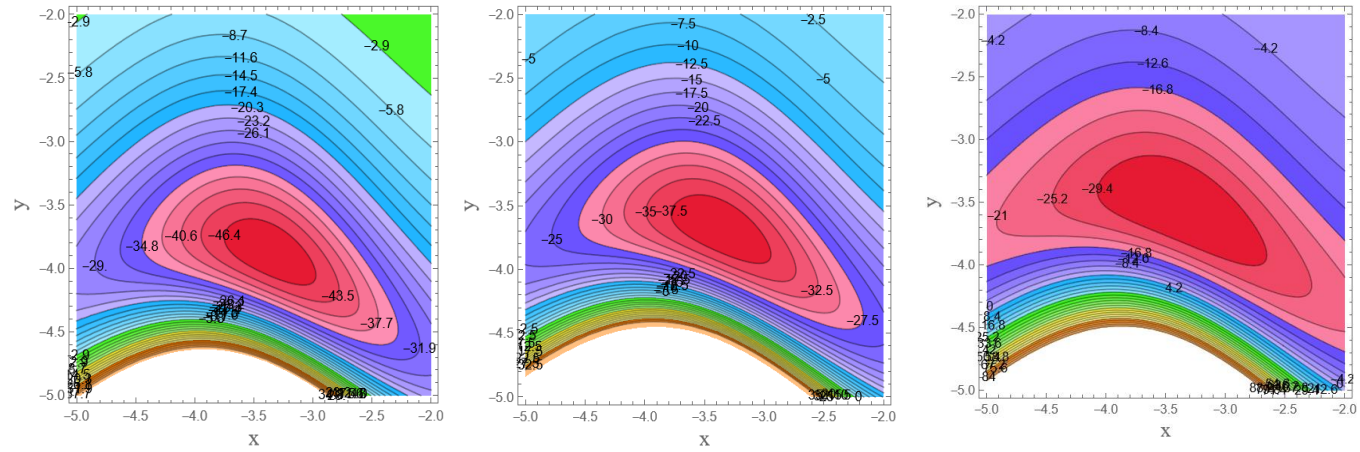

Figure 4. Stream function variation for different (a) $\beta = 2.5$, (b) β=2.6, (c) β=2.7 when $\mathrm{Ha} = 7.5, \mathrm{Da} = 10, \rho = 0.7, d = 5, \Omega = 1.5, \mu = 3, w = 0.01, \phi = 2.5, a = 0.4, b = 0.6, d_1 = 0.5, F_\circ = 0.9, \beta_1 = 4, \alpha = 0.6$

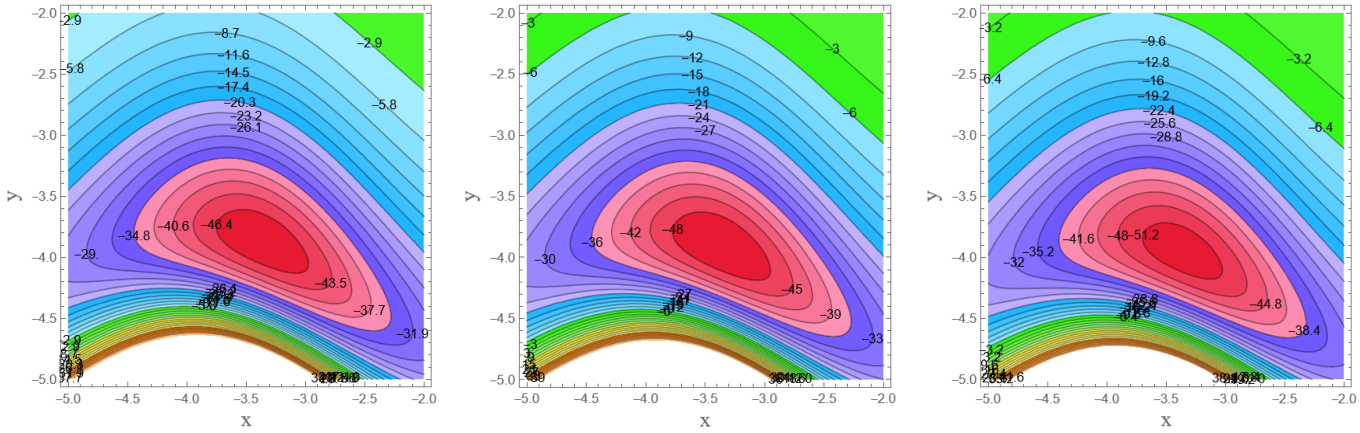

Figure 5. Stream function variation for different (a) $\Omega = 1.5$, (b) Ω=1.55, (c) Ω=1.6 when $\mathrm{Ha} = 7.5, \beta = 2.5, \mathrm{Da} = 10, \rho = 0.7, d = 5, \mu = 3, w = 0.01, \phi = 2.5, a = 0.4, b = 0.6, d_1 = 0.5, F_\circ = 0.9, \beta_1 = 4, \alpha = 0.6$

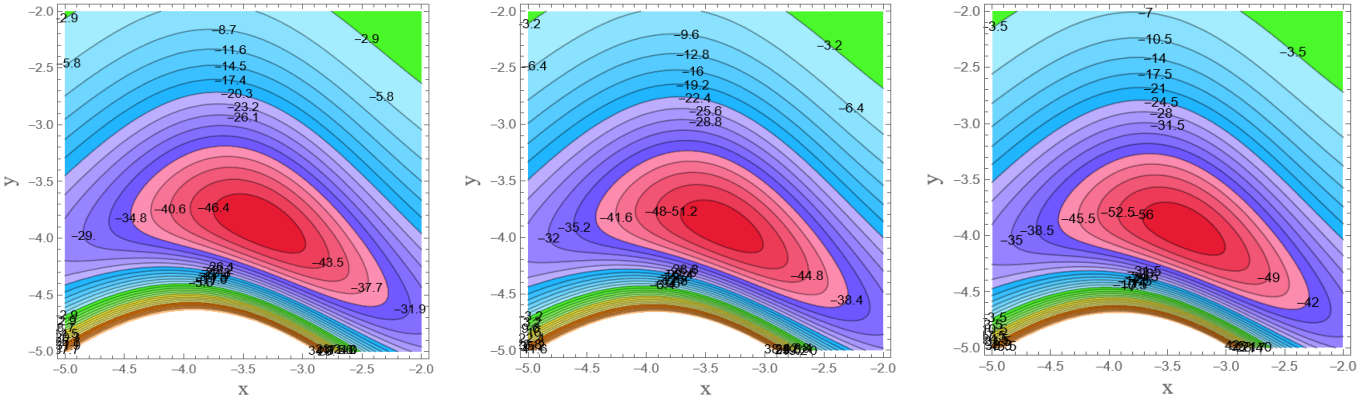

Figure 6. Stream function variation for different (a) w=0.01, (b) w=0.41, (c)w=0.81 when $\mathrm{Ha} = 7.5, \beta = 2.5, \mathrm{Da} = 10, \rho = 0.7, d = 5, \Omega = 1.5, \mu = 3, \phi = 2.5, a = 0.4, b = 0.6, d_1 = 0.5, F_\circ = 0.9, \beta_1 = 4, \alpha = 0.6$

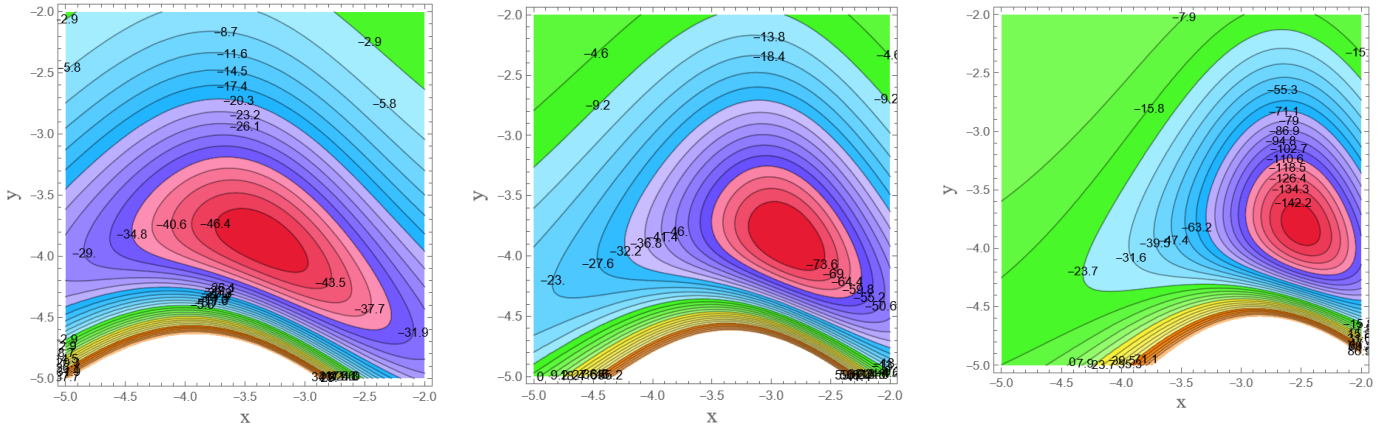

(a) **(b)** **(c)**

Figure 7. Stream function variation for different (a) $\phi = 2.5$, (b) ϕ=2, (c) ϕ=1.5 when Ha $= 7.5, \beta = 2.5$, Da $= 10$, $\rho = 0.7, d = 5, \Omega = 1.5, \mu = 3, w = 0.01, a = 0.4, b = 0.6, d_1 = 0.5, F_\circ = 0.9, \beta_1 = 4, \alpha = 0.6$

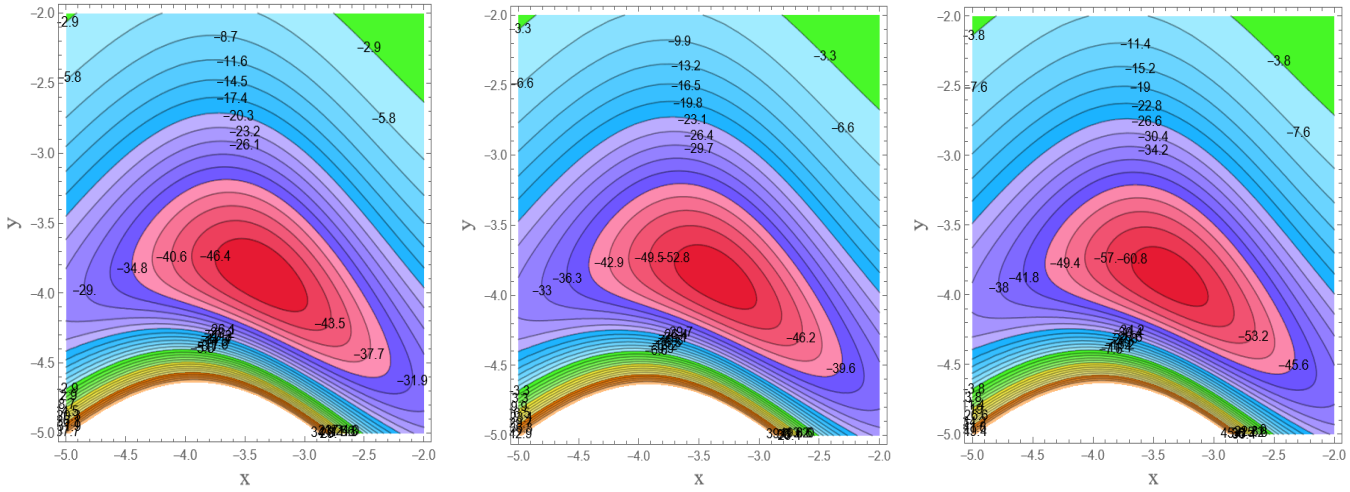

(a) **(b)** **(c)**

Figure 8. Stream function variation for different (a) $\beta_1 = 4$, (b) $\beta_1 = 3.5$, (c) $\beta_1 = 3$ when Ha $= 7.5, \beta = 2.5,$ Da $= 10$, $\rho = 0.7, d = 5, \Omega = 1.5, \mu = 3, w = 0.01, \phi = 2.5, a = 0.4, b = 0.6, d_1 = 0.5, F_\circ = 0.9, \alpha = 0.6$

4.Conclusions

This study examines how coupling stress, slip condition, and rotation affect the peristaltic movement of a Powell-Eyring fluid through a porous medium that is vulnerable to inclined MHD and heat transfer. The asymmetric channel is formed by selecting peristaltic waves with varying amplitudes and phases on the non-uniform walls and a low Reynolds number. The formulas for stream function are produced. Multiple graphs are utilized for parameter analysis:

When the values of the Hartman number (Ha), the inclination of the magnetic field (β), and the couple stress parameter (α) increase leads to an increase in the size of the trapped bolus and approaching the channel wall's, while the increases in the values of the rotation (Ω) and the values of the porous medium parameter (w) led to the decrease in the size of the trapped bolus and move away from the channel walls. While, when the values of the Darcy number (Da) decrease leading to the increase in the size of the trapped bolus and approaching the channel walls, the opposite occurs when the decrease values of the amplitude ratio (ϕ) and the slip condition(β_1).

Acknowledgment

We hereby confirm that all the Figures and Tables in the manuscript are ours. Furthermore, any figures and images, that are not ours, have been included with the necessary permission for republication, which is attached to the manuscript.

Conflict of Interest

The authors declare that they have no conflicts of interest.

Funding

There is no funding for the article.

References

1. Latham TW. Fluid Motion in Peristaltic Pumps. M.S. Thesis, Massachusetts Institute of Technology, 1966.
2. Hina S, Mustafa M, Hayat T, Alsaedi A. Peristaltic flow of Powell-Eyring fluid in curved channel with heat transfer: A useful application in biomedicine. Comput Methods Programs Biomed. 2016;135:89–100. https://doi.org/10.1016/j.cmpb.2016.07.019
3. Hayat T, Aslam N, Rafiq M, Alsaadi FE. Hall and Joule heating effects on peristaltic flow of Powell–Eyring liquid in an inclined symmetric channel. Results in Physics. 2017;7:518–528. https://doi.org/10.1016/j.rinp.2017.01.008
4. Ali HA, Abdulhadi AM. Analysis of heat transfer on peristaltic transport of Powell-Eyring fluid in an inclined tapered symmetric channel with Hall and Ohm's heating influences. J Al-Qadisiyah Comput Sci Math. 2018;10:26–41. https://doi.org/10.29304/jqcm.2018.10.2.364
5. Hussain Q, Alvi N, Latif T, Asghar S. Radiative heat transfer in Powell–Eyring nanofluid with peristalsis. Int J Thermophys. 2019;40:1–20. https://doi.org/10.1007/s10765-019-2510-8
6. Hummady LZ. Effect of couple stress on peristaltic transport of Powell-Eyring fluid peristaltic flow in inclined asymmetric channel with porous medium. Wasit J Comput Math Sci. 2022;1:106–118.
7. Satya Narayana PV, Tarakaramu N, Moliya Akshit S, Ghori J. MHD flow and heat transfer of an Eyring-Powell fluid over a linear stretching sheet with viscous dissipation - A numerical study. Front Heat Mass Transfer (FHMT). 2017;9. https://doi.org/10.5098/hmt.9.9
8. Eldabe NT, Kamel KA, Ramadan SF, Saad RA. Peristaltic motion of Eyring-Powell nano fluid with couple stresses and heat and mass transfer through a porous media under the effect of magnetic field inside asymmetric vertical channel. J Adv Res Fluid Mech Therm Sci. 2020;68:58–71. https://doi.org/10.37934/arfmts.68.2.5871
9. Noreen S, Kausar T, Tripathi D, Ain QU, Lu DC. Heat transfer analysis on creeping flow Carreau fluid driven by peristaltic pumping in an inclined asymmetric channel. Therm Sci Eng Prog. 2020;17. https://doi.org/10.1016/j.tsep.2020.100486
10. Khudair WS, Dwail HH. Studying the magnetohydrodynamics for Williamson fluid with varying temperature and concentration in an inclined channel with variable viscosity. Baghdad Sci J. 2021;18:531. https://doi.org/10.21123/bsj.2021.18.3.0531
11. Salih DG. Influence of varying temperature and concentration on magnetohydrodynamics peristaltic transport for Jeffrey fluid with a nanoparticles phenomenon through a rectangular porous duct. Baghdad Sci J. 2021;18:279. https://doi.org/10.21123/bsj.2021.18.2.0279
12. Ahmed TS. Effect of inclined magnetic field on peristaltic flow of Carreau fluid through porous medium in an inclined tapered asymmetric channel. Al-Mustansiriyah J Sci. 2018;29:94–105. https://doi.org/10.23851/mjs.v29i3.641

13. Mhammad GG. Effect of inclined magnetic field on the peristaltic flow of non-Newtonian fluid with partial slip and couple stress in a symmetric channel. Br J Appl Sci Technol. 2016;15(3).1-11. https://doi.org/10.9734/BJAST/2016/23407
14. Jasim AM. Study of the impact of unsteady squeezing magnetohydrodynamics copper-water with injection-suction on nanofluid flow between two parallel plates in porous medium. Iraqi J Sci. 2022;63:3909–3924. https://doi.org/10.24996/ijs.2022.63.9.23
15. Ali HA. Impact of varying viscosity with Hall current on peristaltic flow of viscoelastic fluid through porous medium in irregular microchannel. Iraqi J Sci. 2022;63:1265–1276. https://doi.org/10.24996/ijs.2022.63.3.31
16. Aziz A, Jamshed W, Aziz T, Bahaidarah H, Ur Rehman K. Entropy analysis of Powell–Eyring hybrid nanofluid including effect of linear thermal radiation and viscous dissipation. J Therm Anal Calorim. 2021;143:1331–1343. https://doi.org/10.1007/s10973-020-10210-2
17. Kareem RS, Abdulhadi AM. Impacts of heat and mass transfer on magneto hydrodynamic peristaltic flow having temperature-dependent properties in an inclined channel through porous media. Iraqi J Sci. 2020;61:854–869. https://doi.org/10.24996/ijs.2020.61.4.19
18. Hage AK, Hummady LZ. Influence of inclined magnetic field and heat transfer on peristaltic transfer Powell-Eyring fluid in asymmetric channel and porous medium. Int J Nonlinear Anal Appl. 2022. https://doi.org/10.22075/ijnaa.2022.6469
19. Mohaisen HN, Abedulhadi AM. Effects of the rotation on the mixed convection heat transfer analysis for the peristaltic transport of viscoplastic fluid in asymmetric channel. Iraqi J Sci. 2022;63:1240–1257. https://doi.org/10.24996/ijs.2022.63.3.29
20. Salih AW. Influence of rotation, variable viscosity and temperature on peristaltic transport in an asymmetric channel. Turk J Comput Math Educ (TURCOMAT). 2021;12:1047–1059.
21. Abdulhussein H, Abdulhadi AM. Impact of couple stress and rotation on peristaltic transport of a Powell-Eyring fluid in an inclined asymmetric channel with Hall and Joule heating. J Basic Sci. 2022;8.
22. Salman MR, Abdulhadi AM. Influence of heat and mass transfer on inclined (MHD) peristaltic of pseudoplastic nanofluid through the porous medium with couple stress in an inclined asymmetric channel. In: J Phys Conf Ser; IOP Publishing; 2018; Vol. 1032, p. 12043. https://doi.org/10.1088/1742-6596/1032/1/012043
23. Gamachu D, Ibrahim W. Entropy production on couple-stress hybrid nanofluid flow in a rocket engine nozzle with non-Fourier's and non-Fick's law. Ain Shams Eng J. 2023;14:101818. https://doi.org/10.1016/j.asej.2022.101818
24. Prasad KV, Choudhari R, Vaidya H, Bhat A, Animasaun IL. Analysis of couple stress nanofluid flow under convective condition in the temperature-dependent fluid properties and Lorentz forces. Heat Transfer. 2023;52:216–235. https://doi.org/10.1002/htj.22692